

**Concentrating ammonium in wastewater by forward osmosis using surface modified nanofiltration membrane**

Journal:	<i>Environmental Science: Water Research &amp; Technology</i>
Manuscript ID	EW-ART-10-2018-000690.R1
Article Type:	Paper
Date Submitted by the Author:	30-Nov-2018
Complete List of Authors:	Jafarinejad, Shahryar; University of California, Irvine, Civil and Environmental Engineering; Tuskegee University College of Engineering Park, Hosung; UC Irvine, Civil and Environ Engineering Mayton, Holly; University of California, Riverside Walker, Sharon; University of California, Riverside, Chemical and Environmental Engineering Jiang, Sunny ; UC Irvine, Civil and Environ Engineering

**Water Impact Statement**

Municipal wastewater contains a high concentration of nitrogen in the form of ammonium, which pollutes the environment if not properly removed before discharging. However, the engineering processes for nitrogen removal are energy intensive. Recovery of ammonium from domestic wastewaters can convert the waste into resources. This study reports concentrating ammonium in the wastewater using a surface modified nanofiltration membrane operating in forward osmosis mode. Ammonium rejection by the modified membranes was greater than 99% for the synthetic ammonium solution.

1 **Concentrating ammonium in wastewater by forward osmosis using surface modified**  
2 **nanofiltration membrane**

3

4 Shahryar Jafarinejad<sup>a,b</sup>, Hosung Park<sup>a</sup>, Holly Mayton<sup>c</sup>, Sharon L. Walker<sup>c</sup>, Sunny C. Jiang<sup>a\*</sup>

5 <sup>a</sup>Department of Civil and Environmental Engineering, University of California, Irvine, CA,  
6 USA

7 <sup>b</sup>Department of Chemical Engineering, College of Engineering, Tuskegee University, Tuskegee,  
8 AL, USA

9 <sup>c</sup>Department of Chemical and Environmental Engineering, University of California, Riverside,  
10 CA, USA

11

12 \*Corresponding author: 844 Engineering Tower, Irvine, CA 92697; Tel: 949-824-5527; email:  
13 sjiang@uci.edu

14

15

16 **Keywords:** Surface modification, Nanofiltration, Ammonium, Forward osmosis

17

## 18 **Abstract**

19 Municipal wastewater contains a high concentration of nitrogen in the form of ammonium,  
20 which pollutes the environment if not properly removed before discharge. However, the energy  
21 intensive processes necessary to convert the biologically available forms of nitrogen into the  
22 unfixed elemental form ( $N_2$ ) during wastewater treatment contradict the costly industrial efforts  
23 to achieve the opposite (i.e. Haber process) for production of nitrogen fertilizers for agricultural  
24 uses. Recovery of ammonium from domestic wastewater should be a priority for wastewater  
25 treatment plants to convert the waste into resources. This study reports developing a surface  
26 modified nanofiltration membrane operating in forward osmosis mode for concentrating  
27 ammonium in wastewater. Surface modification was accomplished using  
28 dicyclohexylcarbodiimide (DCC) as a cross-linking agent to graft polyethylenimine (PEI) on the  
29 polyamide (PA) thin film composite (TFC) membrane. Changes in membrane surface chemical  
30 structure and zeta potential demonstrated the successful incorporation of PEI. The modified  
31 membranes had similar surface roughness to the virgin membrane but improved hydrophilicity.  
32 Filtration tests using synthetic ammonium solutions demonstrated improved water flux and  
33 reduced reverse solutes ( $Mg^{2+}$  and  $Cl^-$  ions) flux in some of the modified membranes. All PEI  
34 grafted membranes had improved ammonium rejection for synthetic ammonium solutions as  
35 well as a secondary return activated sludge sample from a wastewater treatment plant.  
36 Ammonium rejection by the modified membranes was greater than 99% for the synthetic  
37 ammonium solution. The rejection rate declined to 89.3% for treating real wastewater but was  
38 much improved in comparison to 75.5% rejection by the virgin membrane. PEI-modified  
39 membranes present a potential technology for the collection and reuse of ammonium from  
40 wastewater sources.

## 41 **1. Introduction**

42 Domestic and industrial wastewaters contain large amounts of nitrogenous compounds, including  
43 ammonia.<sup>1-6</sup> In fact, up to 40-50% of the total nitrogen in a municipal wastewater treatment  
44 plant is in the form of ammonium ion ( $\text{NH}_4^+$ ).<sup>7</sup> Discharge of these nitrogenous compounds into  
45 the environment can cause eutrophication of the surface waters<sup>8</sup> and toxic effects on aquatic life  
46 even in very low concentrations.<sup>9</sup> To protect aquatic ecosystems and human health, the U.S.  
47 Environmental Protection Agency (EPA) mandates nitrogen removal before wastewater can be  
48 discharged to the environment.<sup>10</sup>

49 Biological treatments that include aerobic nitrification and anaerobic denitrification  
50 processes<sup>11</sup> are the most commonly used approaches to treat wastewater for ammonium removal  
51 in wastewater treatment plants (WWTPs). Both processes are costly in terms of energy,  
52 maintenance, and operation during wastewater treatment. For example, nitrification requires over  
53 four times more oxygen than is needed for organic carbon removal in wastewater.<sup>12</sup> Recently, a  
54 novel process was discovered in which ammonium is converted to dinitrogen gas under anoxic  
55 conditions with nitrite as the electron acceptor. This process, named Anammox (anaerobic  
56 ammonium oxidation), reduces the energy intensity of treatment by short-circuits the nitrification  
57 step.<sup>13, 14</sup> However, the need to convert the biologically available forms of nitrogen into nitrogen  
58 gas remains, which contradicts costly industrial efforts for production of nitrogen fertilizers for  
59 agricultural uses.

60 Therefore, recover the ammonium from domestic wastewater should be a priority for  
61 wastewater treatment plants to convert the waste into resources. So far, there are no cost-effective  
62 methods available to achieve this. Most existing methods that can be used to recover ammonium,  
63 such as air stripping, electrodialysis, struvite precipitation and membrane technologies like

64 reverse osmosis (RO), require the ammonium concentration about 20 times higher than that in  
65 domestic wastewater (40–60 mg/L of  $\text{NH}_4\text{-N}$ ). Therefore, none of the current methods are  
66 economical for ammonium recovery. Here, we propose using a forward osmosis (FO) process to  
67 concentrate the ammonium in the wastewater for down stream recovery.

68 FO follows the natural osmosis gradient for solvent diffusion through membrane from  
69 feed solution (FS) with higher water chemical potential to draw solution (DS) with lower water  
70 chemical potential.<sup>15-19</sup> FO has been proposed for treating complex water matrices due to its low  
71 fouling propensity and low energy requirements.<sup>20, 21</sup> However, past research has found relatively  
72 low rejection of ammonium (48.1±10.5% rejection) in a pilot-scale FO system, despite its high  
73 efficiency in separation of organic matter and phosphorus.<sup>21</sup> This is largely due to the small  
74 molecular weight of ammonium ions, similar to that of water molecules, which are permitted by  
75 diffusion through the membrane. To increase ammonium rejection by FO, membrane properties  
76 have to be improved.

77 Considerable efforts have been made in exploring appropriate FO membranes on ready-  
78 made membranes. Chemical modification has become an important method in novel FO  
79 membrane exploration in recent years.<sup>18, 22</sup> One strategy for improving ammonium rejection is to  
80 create a positively charged, highly hydrophilic membrane surface that repels the positively  
81 charged ammonium ions, while maintaining a greater affinity for the diffusion of water  
82 molecules through membrane. Membrane surface modification has been widely used to improve  
83 membrane properties for various purposes.<sup>23-27</sup> Many efforts have been made to develop new  
84 membranes with positively charged surfaces.<sup>18, 28-32</sup> Among many physical- and chemical-based  
85 surface treatment methods, polyethylenimine (PEI) has shown promise as the aqueous reactant  
86 with polyamine (PA), which forms amine-rich polyamidine layer on thin film composite (TFC)

87 membrane surfaces through interfacial polymerization.<sup>28, 33</sup> Another approach is the use of  
88 carbodiimide-induced grafting with PEI to dramatically improve the hydrophilicity of the  
89 membrane surface, which not only provides a positively charged surface to repel positively  
90 charged ions, but also has excellent antifouling properties due to the membrane hydrophilicity.<sup>33,</sup>  
91 <sup>34</sup>

92 Here, we report surface modification of PA TFC membranes with nanofiltration (NF)  
93 properties. Compared to the typical RO-like FO membranes that are used for brackish water or  
94 seawater desalination applications, the NF-like FO membranes have great potential for organic  
95 wastewater treatment due to their higher water flux.<sup>35, 36</sup> Abdullah et al. (2018)<sup>37</sup> demonstrated  
96 high water flux and minimum reverse solute flux using TFC NF membrane (NF90 and NF270,  
97 Dow FilmTech) in FO mode in treating palm oil mill effluent with divalent salts as the draw  
98 solution. In this study, MgCl<sub>2</sub> was used as the draw solution to evaluate ammonium rejection of  
99 the modified TFC NF membrane in FO mode in synthetic ammonium solution and in return  
100 activated sludge (RAS) from a wastewater treatment plant. The separation performance of the  
101 modified membranes was investigated with regards to permeability, selectivity toward  
102 ammonium ions, as well as the surface physicochemical properties.

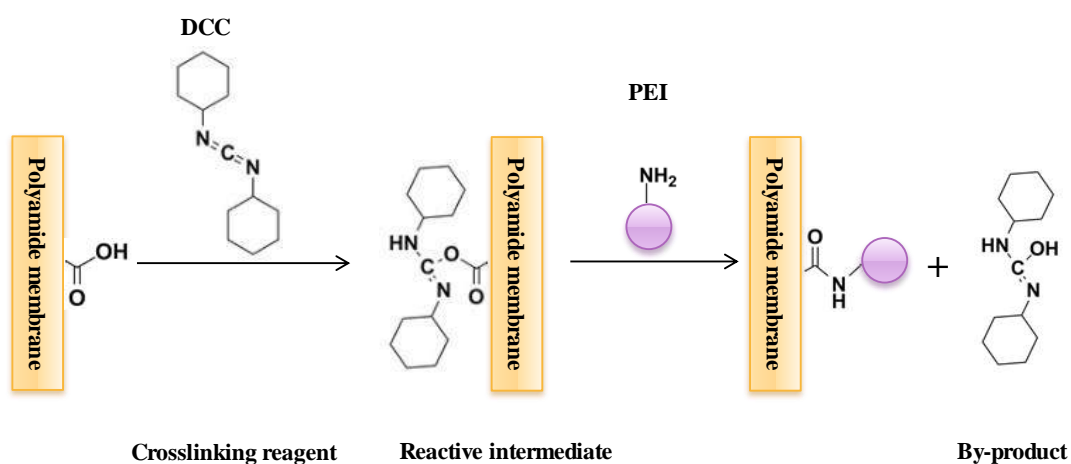
103

## 104 **2. Materials and Methods**

### 105 **2.1. Membrane modification**

106 A PA TFC NF membrane (NFS, molecular weight cutoff of 100-250 Da) from Snyder Filtration,  
107 Inc. was used as the virgin membrane for surface modification. The membrane has approximate  
108 molecular weight cutoff of 100-250Da, minimal MgSO<sub>4</sub> rejection of 99.5% and average NaCl  
109 rejection of 50-55% under 760 kPa operation pressure (Snyder Filtration

110 <http://synderfiltration.com/nanofiltration/nfs-membrane/>). Branched PEI solution with a  
 111 molecular weight (MW) of 70,000 (30 w/v% solution in water), N,N'-dicyclohexylcarbodiimide  
 112 (DCC), dimethylsulfoxide (DMSO), ammonium chloride, and magnesium chloride were  
 113 purchased from Fisher Scientific Inc. and were used without further purification. The proposed  
 114 mechanism for the membrane surface modification is shown in Figure 1. DCC is used to react  
 115 with carboxyl groups on the membrane surface to form a reactive o-acylisourea intermediate,  
 116 which is then displaced by nucleophilic attack from primary amino groups of PEI in the reaction  
 117 medium. The primary amine forms an amide bond with the carboxyl group, and an insoluble  
 118 dicyclohexyl urea (DCU) by-product is generated that can be separated.



119  
 120 Figure 1. Schematic of the membrane surface modification mechanism and process  
 121

122 In preparation for membrane surface modification, DCC (2.9 mmol) was dissolved in  
 123 DMSO (10 part DMSO and 1 part DI water) as the activation solution. PEI was then added to the  
 124 activation solution in various concentrations to form the final grafting solution. Six  
 125 concentrations of PEI, 0.2, 0.6, 1, 1.5, 3, or 4.5% (w/v), was tested for PEI incorporation to PA.  
 126 Since the NFS membrane's polyester support and microporous polysulfone interlayer are  
 127 sensitive to DMSO, the membrane piece was fixed in a 6 cm × 18 cm plate-frame cassette to



128 ensure the reactant solutions only had contact with the PA active layer. A 60 mL grafting  
129 solution was poured onto the membrane surface for reaction at room temperature (22°C) for 15  
130 hours. At the end of incubation, membranes were washed several times with DI water to remove  
131 any unreacted chemicals and finally stored in DI water at 4°C until use. No penetration of  
132 DMSO to the support layer or damage of the support layer was observed during the reaction  
133 period. The modified membranes were named based on the concentration of PEI in the grafting  
134 reaction, for example, reaction with 0.2% PEI is denoted as 0.2% PEI-NFS. The unmodified  
135 Synder's NFS membrane was denoted as the virgin NFS.

136         It is important to mention that before adoption of NFS membrane for surface  
137 modification, we compared NFS membrane and DOW SW30XLE RO membrane (Dow  
138 Filmtec™, Midland, MI) for operation in the FO mode. This preliminary study showed that  
139 under the same osmotic gradient, NFS has averaging 2.7 times greater water flux than  
140 SW30XLE in the FO operation (data not shown). This result agrees with previous work  
141 demonstrating the NF-like FO membrane to produce higher water flux.<sup>36, 37</sup> A HTI FO membrane  
142 (HTI-ES, Albany, USA) was also initially used for comparison but was terminated due to  
143 discontinuing of the product by the manufacturer and the poor ammonia rejection.<sup>20</sup> NFS was  
144 used as the sole membrane for surface modification to demonstrate that surface electrostatic  
145 repulsion plays a major role of ammonium ion rejection instead of the membrane pore size.

## 146 **2.2. Membrane surface characterization**

### 147 **2.2.1. Raman spectroscopy measurement**

148 The membrane surface chemical structure and composition of NFS membrane before and after  
149 modification were determined by a Renishaw InVia Raman microscope in the region of 200–  
150 3,600 cm<sup>-1</sup> to confirm the grafting of PEI onto the membrane surface. The Raman spectra of the

151 virgin NFS membrane and the PEI (liquid solution) were also acquired to identify the PEI signal  
 152 peaks on the modified NFS membrane surfaces. The analysis for PEI solution was performed at  
 153 room temperature with a 532 nm laser as the radiation source under a 10% power of the nominal  
 154 laser intensity and an integration time of 10 s; whereas the analysis for virgin and modified NFS  
 155 membranes was conducted with a 785 nm laser. The baseline was corrected for all spectrums  
 156 using WIRE 3.4 software (Reinshaw). The maximum amount of PEI grafted onto the membrane  
 157 surfaces was determined based on significant differences in the expected PEI signal peak counts.

### 158 **2.2.2. Surface roughness, charge and hydrophilicity measurements**

159 The morphology and surface roughness analyses were carried out by 3D Laser Scanning  
 160 Confocal Microscope (VK-X250, KEYENCE Corporation, USA) at room temperature with  
 161 scanning area of  $10 \times 10 \mu\text{m}^2$ . All the reported surface roughness values are an average obtained  
 162 from three different positions on each membrane.

163 A SurPASS streaming potential analyzer (Anton Paar, Graz, Austria) with an adjustable  
 164 gap cell was used to measure electrokinetic properties of membrane surface. Membranes were  
 165 cut and immobilized on the sample supports ( $20 \text{ mm} \times 10 \text{ mm}$ ) within the cell, and the gap was  
 166 adjusted to approximately  $100 \mu\text{m}$ . The zeta potential ( $\zeta$ ) of each membrane was calculated  
 167 from the streaming potential using the Fairbrother-Mastin approach as follows:

$$168 \quad \zeta = \frac{dU}{dp} \times \frac{\eta}{\varepsilon \times \varepsilon_0} \times \frac{1}{R} \times k_{\text{high}} \times R_{\text{high}} \quad (1)$$

169 where,  $\frac{dU}{dp}$  is the streaming potential coefficient,  $\eta$  is the viscosity of the electrolyte solution,  
 170  $\varepsilon \times \varepsilon_0$  is the dielectric coefficient of the electrolyte solution,  $R$  is the electrical resistance inside the  
 171 streaming channel,  $k_{\text{high}}$  is the electrolyte conductivity and  $R_{\text{high}}$  is the resistance inside the

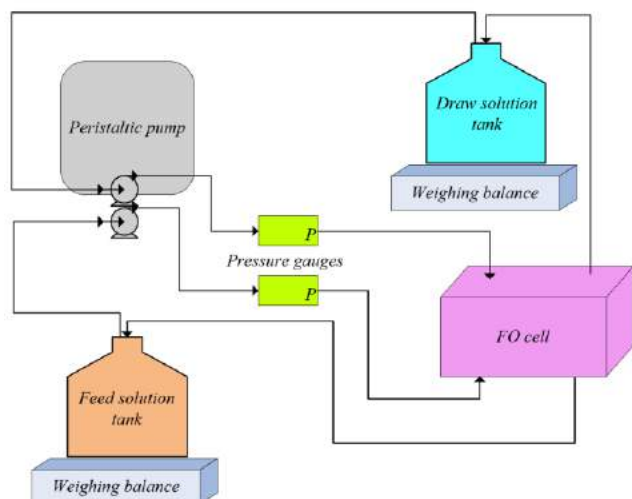
172 streaming channel at high ionic strength.<sup>38</sup> The zeta potential was measured in 1 mM KCl at  
173 room temperature over a pH range of 3 - 9 through titration with 0.5 N NaOH.

174 The hydrophilicity of membrane surfaces was tested using a Goniometer (OPTIXCAM  
175 SUMMIT K2, Rame-Hart, Inc., USA) equipped with a video camera. DI water (1  $\mu$ L) was  
176 placed in six random locations on each membrane sample at room temperature and an image was  
177 acquired of the water droplet. The left and right contact angles were measured using Toup View  
178 Image software. For each sample, six measurements were averaged to get a reliable value.

### 179 **2.3. Membrane filtration properties**

#### 180 **2.3.1. FO operational conditions**

181 A cross flow FO cell (Sterlitech CF042D-FO Cell, USA) was used to test the FO filtration  
182 properties in batch mode (Figure 2). The FO cell had an effective membrane area of 42 cm<sup>2</sup>. In  
183 FO application mode, the active membrane surface was in contact with the feed solution (FS)  
184 and the support layer (back layer) was in contact with draw solution (DS). Both solutions (0.25 L  
185 for DS and 0.5 L for FS) were pumped in the counter-current direction by peristaltic pumps at  
186 flow rate of 60 mL/min at room temperature unless indicated otherwise. The flow rate is within  
187 the laminar region of the Reynolds number to balance the need for pumping energy conservation  
188 and stable permeate flux.<sup>17</sup> For ammonium rejection experiments, 50 ppm NH<sub>4</sub><sup>+</sup> in the form of  
189 NH<sub>4</sub>Cl in DI was used as FS. In all experiments, 1 M magnesium chloride (MgCl<sub>2</sub>) aqueous  
190 solution was used as DS at the beginning of the batch study. Each experiment ran for 28 h,  
191 during which time water flux was determined using a digital balance for changes in water  
192 volume in the FS and DS tanks. The slow progressive dilution of DS by permeate flux occurred  
193 over the experimental period but did not significantly influence the comparison of properties  
194 between modified and un-modified membranes.



195

196 Figure 2. Schematic of the laboratory-scale forward osmosis (FO) system set up.

197 The reverse solutes ( $\text{Mg}^{2+}$  and  $\text{Cl}^-$ ) flux from DS to FS was determined by the initial and  
 198 final volume of FS and the ion concentrations measured by ion chromatography (IC, 940  
 199 Professional IC Vario, Metrohm, USA). For ammonium rejection, ammonium concentrations of  
 200 initial FS before the FO process and final DS after the FO process were measured using IC. In  
 201 addition, the AmVer™ Salicylate Test 'N Tube™ method was also applied for low range (0-2.50  
 202 mg/L  $\text{NH}_3\text{-N}$ , Hach method 10023) and high range (Hach method 10031, 0-50 mg/L  $\text{NH}_3\text{-N}$ )  
 203 ammonia nitrogen using a DR/890 portable colorimeter to calculate the ammonium rejection.

204 In addition to using 50 ppm  $\text{NH}_4^+$  synthetic solution as FS, a return activated sludge  
 205 (RAS) from the secondary clarifier of a local wastewater treatment plant was used as FS to  
 206 evaluate the membrane application to a real environmental sample. The water fluxes, reverse  
 207 solutes ( $\text{Mg}^{2+}$  and  $\text{Cl}^-$  ions) fluxes, and ammonium rejection by the virgin NFS membrane and  
 208 the 1.5% PEI-NFS membrane were compared using 1 M  $\text{MgCl}_2$  solution as DS and a cross flow  
 209 rate of 60 mL/min at 25 °C.

### 210 2.3.2. Filtration property calculations

211 The water flux across the FO membrane was calculated using the following equation<sup>39-41</sup>:

$$212 \quad J_w = \frac{\Delta V}{A_m \cdot \Delta t} = \frac{\Delta m}{\rho \cdot A_m \cdot \Delta t} \quad (2)$$

213 where,  $J_w$  is the water flux ( $L/m^2 \cdot h$  or  $LMH$ ),  $\Delta V$  (L) is the volume change of DS over time  
 214 interval  $\Delta t$  (h),  $A_m$  ( $m^2$ ) is the effective membrane area,  $\rho$  is the density of the DS ( $g/L$ ), and  $\Delta m$   
 215 (g) is the weight change of the DS. The reverse solutes flux takes place from DS in the reverse  
 216 direction of the water flux and is calculated with the following equation<sup>39</sup>:

$$217 \quad J_s = \frac{C_t V_t - C_0 V_0}{A_m \cdot \Delta t} \quad (3)$$

218 where,  $J_s$  is the reverse solute flux ( $g/m^2 \cdot h$  or  $gMH$ ),  $C_0$  ( $g/L$ ) and  $V_0$  (L) are the initial  
 219 concentration of solutes and initial volume of the FS, respectively.  $C_t$  ( $g/L$ ) and  $V_t$  (L) are the  
 220 solutes concentration and the volume of the FS measured at time of  $t$ , respectively.

221 The ammonium rejection percent (R%) by the membrane was calculated using the  
 222 following equation<sup>20, 32</sup>:

$$223 \quad R(\%) = \left( 1 - \frac{C_p}{C_f} \right) \times 100 \quad (4)$$

224 where,  $C_p$  and  $C_f$  are the ammonium concentration permeated through membrane from FS to DS  
 225 and initial ammonium concentration in FS before FO process, respectively.

226

## 227 **3. Results and discussion**

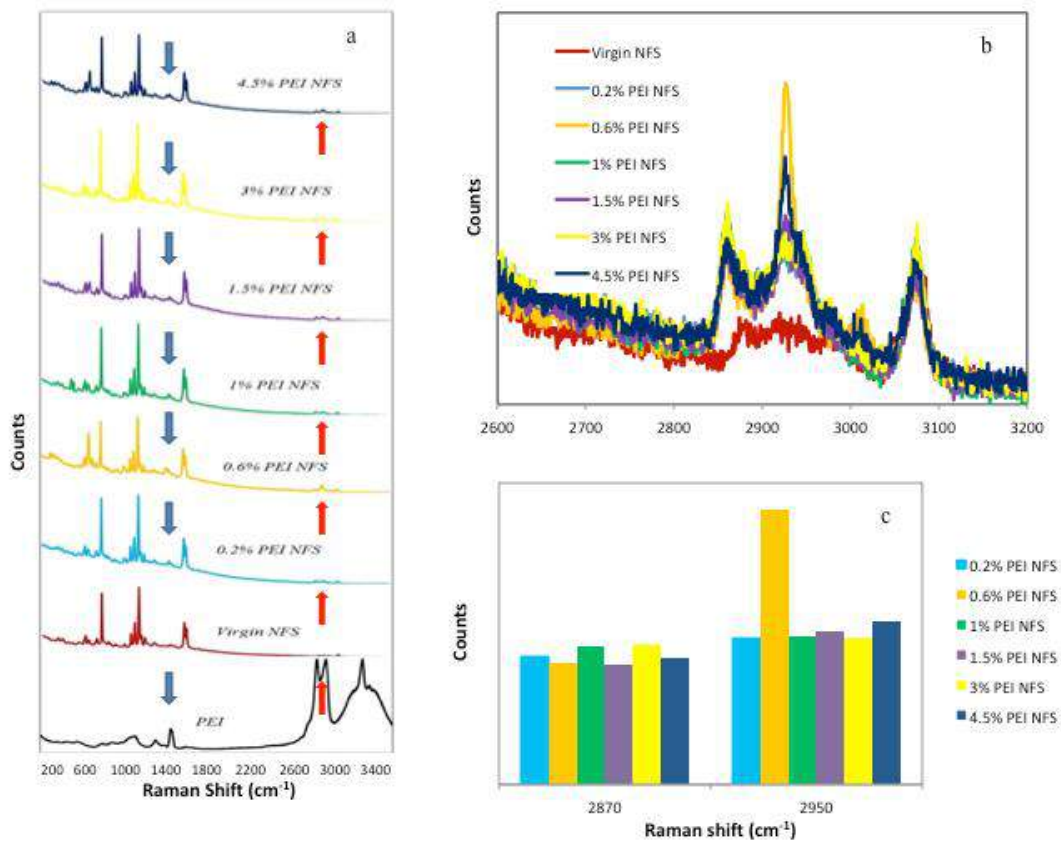
### 228 **3.1. Characterization of membranes**

#### 229 **3.1.1. Raman spectroscopy analysis**

230 Changes of chemical groups on surface modified NFS membranes compared to the virgin NFS  
 231 membrane are shown in Figure 3. Raman spectra of PEI solution have characteristic peaks at  
 232 1460, 2873, 2956, and 3309  $cm^{-1}$ . The bands at 1460 and 3309  $cm^{-1}$  correspond to  $CH_2$

233 deformation vibration and N-H vibration, respectively; whereas the bands at 2873 and 2956  $\text{cm}^{-1}$   
234 are assigned to the C-H vibration.<sup>42</sup> Raman spectra of the virgin NFS membrane has major  
235 spectral peaks located at Raman shifts of 792, 1076, 1111, 1150, 1589, and 1611  $\text{cm}^{-1}$ , which are  
236 likely associated with the polyamide functional groups.<sup>43</sup> Specifically, the bands at 792, 1589,  
237 and 1611  $\text{cm}^{-1}$  are associated with the asymmetric C-N-C stretch of tertiary amides, aromatic in-  
238 plane ring bending vibration, and aromatic amide groups, respectively; whereas, the bands at  
239 1076, 1111, and 1150  $\text{cm}^{-1}$  are assigned to the C-N stretching vibrations of both the piperazine  
240 rings and the amide groups.<sup>39</sup>

241         Compared with the virgin NFS membrane, all the PEI modified NFS membranes have  
242 peaks formation at approximately 1460, 2870 and 2950  $\text{cm}^{-1}$  (Figure 3a, b), which are consistent  
243 with peaks belonging to PEI in its natural state (liquid solution). This result indicates that PEI  
244 was successfully grafted onto the NFS membrane. In addition, as shown in Figure 3c, the counts  
245 or intensity of 2873 and 2956  $\text{cm}^{-1}$  peaks change with the variation of PEI concentration in  
246 grafting solution. The amount of PEI grafted onto the membrane surface is determined by Raman  
247 spectroscopy based on the PEI signal peak counts (Figure 3c). It seems that the PEI  
248 concentrations as low as 0.6% (w/v) are suitable for grafting solutions.



249

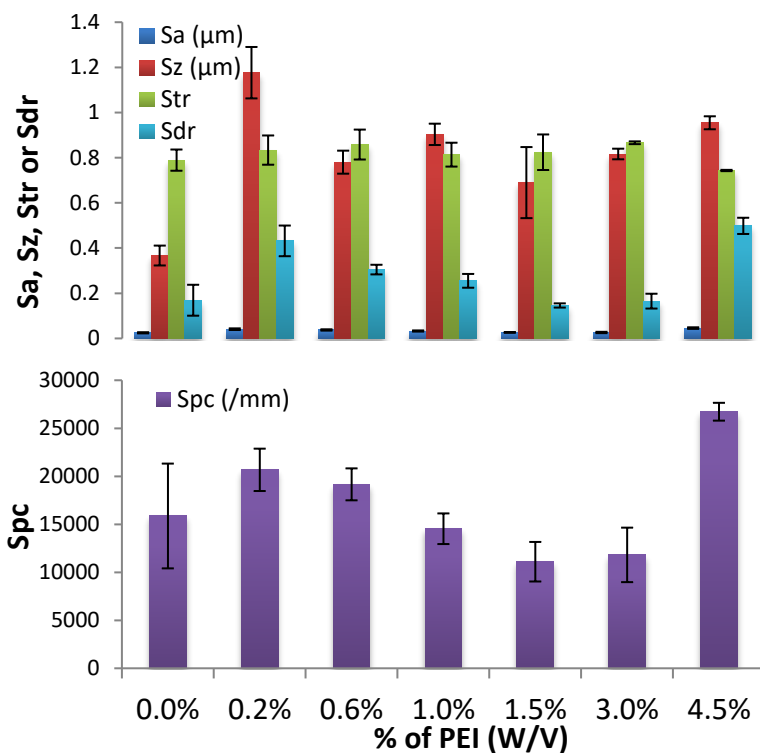
250 Figure 3. Raman spectra of PEI solution, virgin NFS membrane, and PEI grafted NFS  
 251 membranes (a), and an overlay image that compares Raman shift of 2,600 - 3,200  $\text{cm}^{-1}$  (b). The  
 252 PEI signal peak area on membrane surface is quantified in (c). Arrows on (a) indicate the new  
 253 peaks identified on membrane surface that correspond to PEI peaks.

254

### 255 3.1.2. Membranes surface roughness

256 Five surface roughness measurements, including arithmetic mean height ( $S_a$ ), maximum height  
 257 of the surface ( $S_z$ ), texture aspect ratio ( $S_{tr}$ ), arithmetic mean peak curvature ( $S_{pc}$ ), and  
 258 developed interfacial area ratio ( $S_{dr}$ ), were used to compare the virgin NFS membrane and PEI  
 259 grafted NFS membranes (Figure 4). The results confirm that both the virgin NFS membrane and  
 260 PEI grafted NFS membranes have relatively uniform surfaces.  $S_z$  values are slightly higher by

261 PEI grafting on the surface of PA membrane. Sdr and Spc are also greater for 4.5% PEI-NFS  
 262 membrane ( $p < 0.05$ ) but are not significantly different for other PEI grafted NFS membranes in  
 263 comparison with the virgin membrane ( $p > 0.05$ ). This result suggests 4.5% PEI-NFS membrane  
 264 likely become rougher than the virgin membrane. But there is no significant difference in other  
 265 roughness measurements of the modified membranes when compared with the unmodified  
 266 membrane.



267  
 268 Figure 4. The surface roughness measurement (arithmetic mean height (Sa), maximum height of  
 269 the surface (Sz), texture aspect ratio (Str), arithmetic mean peak curvature (Spc), and developed  
 270 interfacial area ratio (Sdr) of the virgin NFS membrane and PEI grafted NFS membranes.

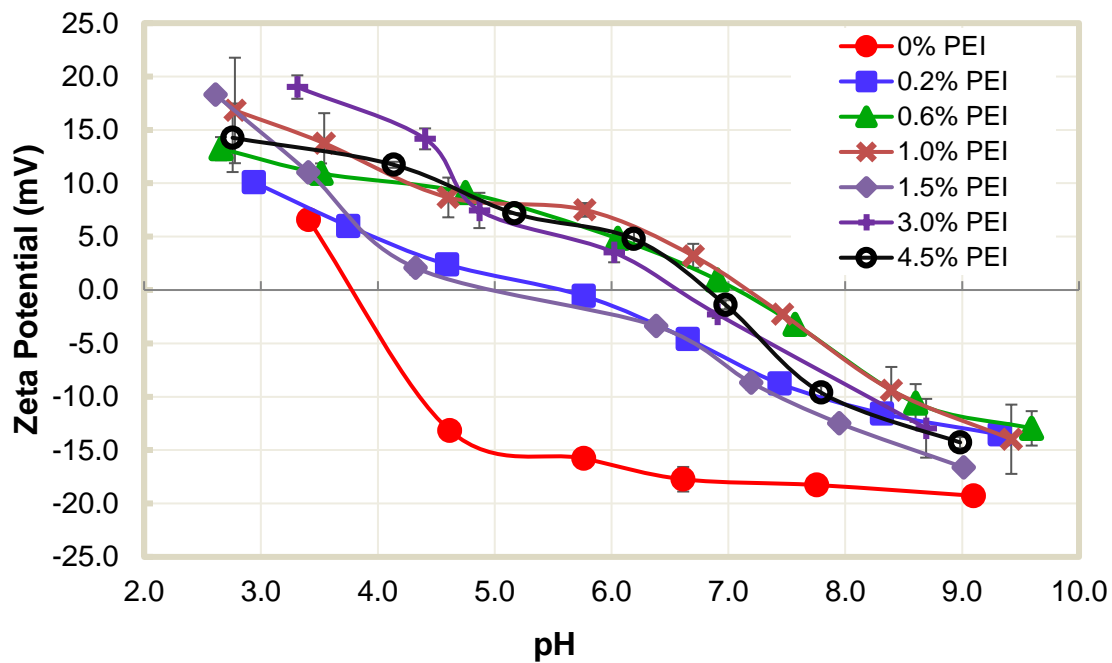
271

### 272 3.1.3. Membranes surface charge

273 The zeta potential measurements of the virgin NFS membrane and PEI grafted NFS membranes  
 274 as a function of pH are shown in Figure 5. The isoelectric point (IEP) for each membrane is



275 indicated by the horizontal line crossing zero zeta potential. The virgin NFS membrane has an  
276 IEP of 3.75. After the PEI grafting, the IEP for the PEI grafted NFS membranes are shifted to  
277 higher values due to increases in positively charged amine groups attached to the surface. These  
278 positive charge groups can be useful for improving ammonium rejection under a range of  
279 environmental conditions. The changes in surface charge on the membrane is best explained by  
280 amine protonation at pH values below the IEP, while increasing pH beyond the IEP results in  
281 deprotonation of carboxyl groups and a negative surface charge as shown by previous  
282 literatures.<sup>33, 35, 44</sup>



283  
284 Figure 5. Zeta potential of the virgin NFS membrane and PEI grafted NFS membranes as a  
285 function of pH.

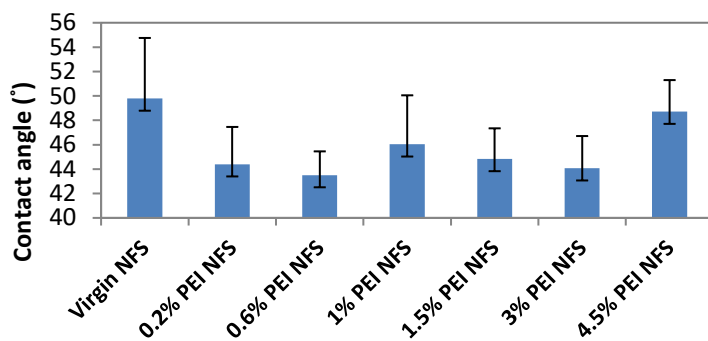
286

287 In all pH ranges, the zeta potential values of the PEI grafted NFS membranes are higher  
288 than that of the virgin NFS membrane. This indicates that the PEI grafted NFS membranes have  
289 more positively charged molecules in comparison with the virgin membrane. At pH value <5.5,

290 all modified membranes displayed net positive charge on surface. At the  $\text{pH} > 5.5$ , the additional  
291 amine groups on membrane surface may translate into higher electrostatic repulsion of  
292 ammonium in comparison with the virgin NFS membrane.

#### 293 **3.1.4. Membranes water contact angle**

294 The hydrophilicity of the membrane can affect its flux and antifouling ability.<sup>32,33</sup> Comparisons  
295 of membrane surface hydrophilicity using water contact angle of the virgin and modified NFS  
296 membranes (Figure 6) indicate that water contact angle of the virgin NFS membrane is  $49.79^\circ$ ,  
297 which is greater than all the PEI grafted NFS membranes. An average value for all PEI grafted  
298 member is  $45.25^\circ$ , in which 0.6% PEI-NFS membrane has the lowest contact angel of  $43.51^\circ$  and  
299 4.5% PE-NFS membrane has the contact angle of  $48.71^\circ$ . Lower water contact angles illustrate  
300 that more water molecules can penetrate into the membrane surface and thus greater  
301 hydrophilicity of the membrane surface. Both the chemical composition and the surface  
302 geometrical structure govern the wettability of a solid surface.<sup>33,45</sup> Therefore, the introduction of  
303 exposed polar groups (amine groups) on the membrane surface likely improved surface  
304 hydrophilicity after the PEI grafting.<sup>33</sup> These results are in agreement with the Raman  
305 spectroscopy data and zeta potential results, confirming the grafting of PEI on the PA NFS  
306 membrane surface. On the other hand, the higher water contact angel observed on 4.5% PEI-NFS  
307 membrane may be explained by the increased roughness of the membrane surface as shown by  
308 the surface roughness measurements in spite of the addition of polar groups on membrane  
309 surface.



310

311 Figure 6. Water contact angle of the virgin NFS membrane and PEI grafted NFS membranes

312

313 **3.2. Membranes filtration performance**

314 The ideal FO membrane should have no reverse solute flux and a high water flux. Reverse solute

315 flux can cause internal concentration polarization (ICP) and membrane fouling.<sup>39, 46</sup> Solute flux316 also decreases the osmotic pressure difference across FO membranes.<sup>18</sup> Comparisons of the317 membrane filtration performance for the water fluxes and reverse solutes ( $Mg^{2+}$  and  $Cl^{-}$  ions)

318 fluxes of the virgin NFS membrane and the PEI grafted NFS membranes are shown in Figure 7.

319 The water flux of the virgin NFS membrane was  $\sim 0.70$  L/m<sup>2</sup>.h at the cross flow rate of 60

320 mL/min. Three of six PEI modified membrane showed improved water fluxes but overall the

321 water fluxes of the PEI modified NFS membranes ranged between 0.37 and 1.32 L/m<sup>2</sup>.h. The

322 variation of water flux may be caused by two conflicting factors associated with PEI grafting.

323 First, the improvement of membrane surface hydrophilicity by PEI incorporation can facilitate

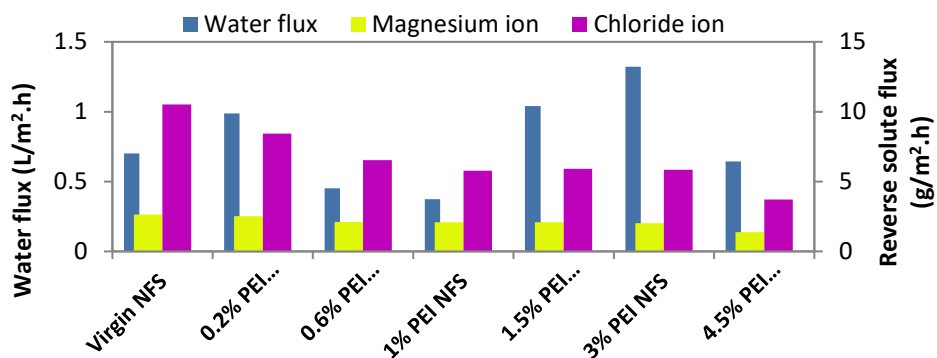
324 water molecules' penetration into membranes that leads to the increase of membrane water flux.

325 Second, the addition of PEI on PA can block membrane pores and increase trans-membrane

326 resistance of water molecules, which results in a reduction of water flux. Thus, the final variation

327 of water flux can depend on which of these two factors dominates.<sup>32, 33, 47</sup>

328



329

330 Figure 7. Water fluxes and reverse solutes ( $Mg^{2+}$  and  $Cl^-$  ions) fluxes of the virgin NFS

331 membrane and the PEI grafted NFS membranes.

332

333 The best water flux is found in 3% PEI-NFS membrane, which has the improved surface

334 smoothness (Figure 4), increased positive charges (Figure 5) and enhanced hydrophilicity

335 (Figure 6). The 1.5% PEI grafted membrane has the second best water flux, smoothness and

336 hydrophilicity. Therefore, 1.5% to 3% of PEI may be the ideal condition for membrane surface

337 modification. It was also noted that the water flux rate observed in this study is slightly lower

338 than a previous study reported by Cornelissen et al.<sup>48</sup> using a similar type of membrane.

339 However, that study was carried out in a much faster cross flow rate (nearly 100 times higher)

340 and using a higher concentration of drawn solution.

341 As shown in Figure 7, the reverse solutes ( $Mg^{2+}$  and  $Cl^-$  ions) fluxes of the virgin NFS

342 membrane are higher than those of the PEI grafted NFS membranes. This result suggests the

343 PEI-NFS membranes have improved properties for reducing reverse solute flux. In addition, the

344 reverse solutes ( $Mg^{2+}$  and  $Cl^-$  ions) fluxes were reduced in general with increasing PEI

345 concentration from 0.2% to 4.5% (Figure 7). Lower reverse solute fluxes can avoid the osmotic

346 pressure decrease caused by reverse solute diffusion and decline in water flux.<sup>18</sup> Furthermore, the347 nanopore size plays a key role in reverse solute flux. The  $Cl^-$  ion reverse diffusion from DS to FS

348 is approximately three times higher than that of  $Mg^{2+}$  ion due to different membrane selectivity  
 349 to monovalent vs. divalent ions (Figure 7).

350 The ratio of water flux,  $J_w$ , to reverse solutes ( $Mg^{2+}$  and  $Cl^-$  ions) flux,  $J_s$ , in the FO  
 351 process (called the reverse solute flux selectivity) is commonly used to quantify the FO  
 352 performances.<sup>49</sup> Table 1 compares the reverse solutes ( $Mg^{2+}$  and  $Cl^-$  ions) flux selectivity of the  
 353 virgin NFS membrane and the PEI grafted NFS membranes at experimental conditions of 1 M  
 354  $MgCl_2$  solution as DS, flow rate of 60 mL/min, and room temperature (25 °C). These results  
 355 confirm that the PEI grafted NFS membranes have improved reverse flux selectivity in  
 356 comparison with virgin membrane in most cases.

357 Table 1. Comparison of the reverse solutes ( $Mg^{2+}$  and  $Cl^-$  ions) flux selectivity of the virgin NFS  
 358 membrane and the PEI grafted NFS membranes

Membrane sample	The reverse solute ( $Mg^{2+}$ ion) flux selectivity (L/g)	The reverse solutes ( $Cl^-$ ion) flux selectivity (L/g)
Virgin NFS	0.266	0.0667
0.2% PEI NFS	0.392	0.1173
0.6% PEI NFS	0.214	0.0691
1% PEI NFS	0.179	0.0648
1.5% PEI NFS	0.498	0.1758
3% PEI NFS	0.658	0.2257
4.5% PEI NFS	0.464	0.1726

359  
 360 When comparing ammonium rejection of PEI grafted membranes with virgin NFS  
 361 membrane using pure  $NH_4Cl$  solution, the results showed that the virgin NFS membrane has  
 362 relatively high ammonium rejection rate (~97%) when operating in the FO mode in comparison  
 363 with previous reports of ammonium rejection in FO operation using TFC embedded polyester  
 364 screen supported HTI-ES membrane (35.8%).<sup>20</sup> Grafting of PEI on NFS membrane further  
 365 improved the ammonium rejection by additional 2-3% for the synthetic ammonium solution  
 366 without exception.

367 To test the applicability of PEI-NFS membranes for concentrating ammonium in real  
 368 wastewater, 1.5% PEI-NFS membrane was compared with virgin NFS membrane using RAS  
 369 from secondary clarifier of a local wastewater treatment plant. The measured characteristics of  
 370 RAS are given in Table 2. Ammonium rejections by the virgin NFS membrane was decreased to  
 371 75.5% for treating the RAS but the PEI-NFS faired better with an average of 89.3% ammonium  
 372 rejection. This increase in ammonium rejection may be explained by repulsion due to the  
 373 increased positively charged molecules on membrane surface from the PEI grafting. The reverse  
 374 solute fluxes of 1.5% PEI NFS membrane (2.43 g/m<sup>2</sup>.h for Mg<sup>2+</sup> ions and 10.04 g/m<sup>2</sup>.h for Cl<sup>-</sup>  
 375 ions) were also much lower than those of the virgin NFS membrane (3.19 g/m<sup>2</sup>.h for Mg<sup>2+</sup> ions  
 376 and 15.72 g/m<sup>2</sup>.h for Cl<sup>-</sup> ions). However, water flux of the virgin NFS membrane (0.58 L/m<sup>2</sup>.h)  
 377 was slightly higher than that of the 1.5% PEI NFS membrane (0.34 L/m<sup>2</sup>.h). Membrane fouling  
 378 was suspected but was not confirmed.

379 Table 2. The characteristics of RAS from secondary clarifier of a local wastewater treatment  
 380 plant

Parameter	Value
Total dissolved solids (TDS)	1295 mg/L
Total suspended solids (TSS)	4306 mg/L
NH <sub>4</sub> <sup>+</sup>	65.231 mg/L
Mg <sup>2+</sup>	56.005 mg/L
Cl <sup>-</sup>	144.343 mg/L

381  
 382 The availability of appropriate FO membranes is crucial to the development of FO  
 383 technology. Problems, such as high reverse solute diffusion and high concentration polarization  
 384 (CP) are frequently encountered in FO processes.<sup>18</sup> Meanwhile, although FO has a lower  
 385 membrane fouling propensity than the pressure-driven membrane processes, fouling is still the  
 386 most severe problem adversely influencing FO performance. Many novel FO membranes  
 387 obtained through the surface modifications on ready-made membranes have been developed in

388 recent years (see review by Xu et al.<sup>18</sup>). The work presented here adds to the body of work in  
389 attempt to develop a FO membrane that has high water flux, low reverse solute flux and high  
390 ammonia rejection. The modified membrane is far from ideal for ammonia concentration. We  
391 have not addressed the membrane fouling, which is a universal challenge in all membrane  
392 processes. The presence of positive charged groups on membrane surface may attract negatively  
393 charged molecules in wastewaters, which exacerbate the fouling propensity. Future work to  
394 further improve the surface hydrophilicity may further improve the membrane antifouling  
395 properties. The work presented here offers a potential new application of FO in converting  
396 ammonia from waste to resources.

397

#### 398 **4. Conclusions**

- 399 • We have successfully grafted PEI as functional groups on PA TFC NF membranes using  
400 DCC intermediate, as demonstrated by Raman spectroscopy.
- 401 • Most of modified membrane maintained the uniform surfaces with minimal changes in  
402 surface roughness in comparison with the virgin membrane.
- 403 • The PEI grafted NFS membranes have higher IEP than virgin membrane due to increases  
404 in amine groups attached to the membrane surface.
- 405 • Most of the PEI grafted NFS membranes had lower water contact angles in comparison  
406 with the virgin NFS membrane, indicating hydrophilicity.
- 407 • The water flux of PEI modified membranes varied among different concentrations of PEI  
408 incorporation, with some having greater water flux than the virgin NFS membrane, while  
409 the fluxes were reduced for others.

- 410       • The reverse fluxes of the PEI-NFS membrane for  $Mg^{2+}$  and  $Cl^{-}$  ions were reduced in  
411       comparison with the virgin membrane.
- 412       • With consideration of the water fluxes, reverse solutes ( $Mg^{2+}$  and  $Cl^{-}$  ions) fluxes and  
413       ammonium rejection, the 1.5% and 3% PEI NFS are considered the best overall  
414       performer.
- 415       • Improvement of ammonium rejection and the reverse solutes ( $Mg^{2+}$  and  $Cl^{-}$  ions) fluxes  
416       by 1.5% PEI-NSF was also demonstrated using RAS of a local wastewater treatment  
417       plant .
- 418
- 419



420 **Acknowledgements:** Funding support for this research was partial provided by U.S./China  
421 Clean Energy Research Center for Water-Energy Technologies program (DE-IA0000018) to  
422 UCI. We would also like to express our gratitude towards the Orange County Sanitation District  
423 for their support of wastewater sample collection and monitoring data. We thank the facility  
424 directors at the Laser Spectroscopy and Optical Biological Core Facilities at the University of  
425 California, Irvine for their guidance of the spectroscopy and microscopy work.

426 **References**

- 427 1. S. Jafarinejad, Cost estimation and economical evaluation of three configurations of activated  
428 sludge process for a wastewater treatment plant (WWTP) using simulation, *Appl. Wat. Sci.*,  
429 2017, **7**, 2513-2521.
- 430 2. S. Jafarinejad, Petroleum waste treatment and pollution control, First edition, Elsevier Inc.,  
431 Butterworth-Heinemann, USA, 2017.
- 432 3. T.J. Van der Weerden, S.C. Jarvis, Ammonia emission factors for N fertilizers applied to two  
433 contrasting grassland soils, *Environ. Pollut.*, 1997, **95**, 205-211.
- 434 4. M.A. Sutton, U. Dragosists, Y.S. Tang, D. Fowler, Ammonia emissions from nonagricultural  
435 sources in the UK, *Atmos. Environ.*, 2000, **34**, 855-869.
- 436 5. H.Y. Fang, M.S. Chou, C.W. Huang, Nitrification of ammonia-nitrogen in refinery  
437 wastewater, *Water Res.*, 1993, **27**, 1761-1765.
- 438 6. C. Korzenowski, M. Minhalma, A.M. Bernardes, J.Z. Ferreira, M.N. Pinho, Nanofiltration for  
439 the treatment of coke plant ammoniacal wastewaters, *Sep. Purif/ Technol.*, 2011, **76**, 303-307.
- 440 7. A. Bodalo, J.L. Gomez, E. Gomez, G. Leon, M. Tejera, Ammonium removal from aqueous  
441 solutions by reverse osmosis using cellulose acetate membranes, *Desalination*, 2005, **184**, 149-  
442 155.
- 443 8. G. Furer, B. Wehrli, Microbial reactions, chemical speciation, and multicomponent diffusion  
444 in porewaters of a eutrophic lake, *Geochim, Cosmochim Act.*, 1996, **60**, 2333-2346.
- 445 9. I. Koyuncu, Effect of operating conditions on the separation of ammonium and nitrate ions  
446 with nanofiltration and reverse osmosis membranes, *J. Environ. Sci. Health, Part A.*, 2002, **37(7)**,  
447 1347-1359.

- 448 10. United States Environmental Protection Agency (US EPA), 2009, Nutrient control design  
449 manual, State of technology review report, Office of research and development, National risk  
450 management research laboratory – Water supply and water resources division, EPA/600/R-  
451 09/012.
- 452 11. R. Sedlack, Phosphorous and Nitrogen removal from municipal wastewater: Principles and  
453 practice, Second ed., Lewis Publisher, New York, 1991.
- 454 12. H. Odegaard, A road-map for energy-neutral wastewater treatment plants of the future based  
455 on compact technologies (including MBBR), *Frontiers of Environmental Science & Engineering*,  
456 2016, **10**:2
- 457 13. Z. Hu, T. Lotti, M. de Kreuk, R. Kleerebezem, M. van Loosdrecht, J. Kurit, M.S. Jetten, B.  
458 Kartal, Nitrogen Removal by a Nitritation-Anammox Bioreactor at Low Temperature, *Appl.*  
459 *Environ. Microb.*, 2013, **79**, 2807-2812.
- 460 14. J.D. Vela, L.B. Stadler, K.J. Martin, L. Raskin, C.B. Bott, N.G. Love, Prospects for  
461 biological nitrogen removal from anaerobic effluents during mainstream wastewater treatment,  
462 *Environ. Sci. Tech Lett.*, 2015, **2**, 234-244.
- 463 15. T.Y. Cath, A.E. Childress, M. Elimelech, Forward osmosis: principles, applications, and  
464 recent developments, *J. Membr. Sci.*, 2006, **281**, 70-87.
- 465 16. T.S. Chung, X. Li, R.C. Ong, Q. Ge, H. Wang, G. Han, Emerging forward osmosis (FO)  
466 technologies and challenges ahead for clean water and clean energy applications, *Curr. Opin.*  
467 *Chem. Eng.*, 2012, **1**, 246-257.
- 468 17. A. Deshmukh, N.Y. Yip, S. Lin S., Elimelech, Desalination by forward osmosis: Identifying  
469 performance limiting parameters through module-scale modeling, *J. Membr. Sci.* 2015, **491**,  
470 159–167.

- 471 18. W. Xu, Q. Chen, Q. Ge, Recent advances in forward osmosis (FO) membrane: Chemical  
472 modifications on membranes for FO processes, *Desalination*, 2017, **419**, 101-116.
- 473 19. S. Zhao, L. Zou, C.Y. Tang, D. Mulcahy, Recent developments in forward osmosis:  
474 opportunities and challenges, *J. Membr. Sci.*, 2012, **396**, 1-21.
- 475 20. Y.P. Devia, T. Imai, T. Higuchi, A. Kanno, K. Yamamoto, M. Sekine, T.V. Le, Potential of  
476 magnesium chloride for nutrient rejection in forward osmosis. *J. Water Resource Protec.*, 2015,  
477 **7**, 730-740.
- 478 21. Z. Wang, J. Zheng, J. Tang, X. Wang, Z. Wu, A pilot-scale forward osmosis membrane  
479 system for concentrating low-strength municipal wastewater: performance and implications,  
480 *Scientific Rep.*, 2016, **6**:21653 DOI: 10.1038/srep21653
- 481 22. D. Rana, T. Matsuura, Surface modifications for antifouling membranes, *Chem. Rev.*, 2010,  
482 **110**, 2448-2471.
- 483 23. A.A. Abuhabib, A. Mohammad, N. Hilal, R.A. Rahman, A.H. Shafie, Nanofiltration  
484 membrane modification by UV grafting for salt rejection and fouling resistance improvement for  
485 brackish water desalination, *Desalination*, 2012, **295**, 16-25.
- 486 24. A.A. Abuhabib, Modified nanofiltration membranes performance improvement for  
487 desalination applications, *INTECH*, 2015, <http://dx.doi.org/10.5772/60212>
- 488 25. M.N. Abu Seman, M. Khayet, Z.I. Bin Ali, N. Hilal, Reduction of nanofiltration membrane  
489 fouling by UV-initiated graft polymerization technique, *J. Membr. Sci.*, 2010, **355**, 133-141.
- 490 26. E.M.V. Wagner, A.C. Sagle, M.M. Sharma, Y.H. La, B.D. Freeman, Surface modification of  
491 commercial polyamide desalination membranes using poly(ethylene glycol) diglycidyl ether to  
492 enhance membrane fouling resistance, *J. Membr. Sci.*, 2011, **367**, 273-287.

- 493 27. Y. Zhou, S. Yu, C. Gao, X. Feng, Surface modification of thin film composite polyamide  
494 membranes by electrostatic self deposition of polycations for improved fouling resistance, Sep.  
495 Purif. Technol., 2009, **66**(2), 287-294.
- 496 28. A. Akbari, Z. Fakharshakeri, S.M.M. Rostami, A novel positively charged membrane based  
497 on polyamide thin-film composite made by cross-linking for nanofiltration, Water Sci. Technol.,  
498 2016, **73.4**, 776-789.
- 499 29. R. Du, J. Zhao, Properties of poly (*N,N*-dimethylaminoethyl methacrylate)/polysulfone  
500 positively charged composite nanofiltration membrane, J. Membr. Sci., 2004, **239**, 183-188.
- 501 30. A.M.S. Jubera, J.H. Herbison, Y. Komaki, M.J. Plewa, J.S. Moore, D.G. Cahill, B.J.  
502 Mariñas, Development and performance characterization of a polyamide nanofiltration  
503 membrane modified with covalently bonded aramide dendrimers, Environ. Sci. Technol., 2013,  
504 **47**, 8642-8649.
- 505 31. M. Li, Z. Lv, J. Zheng, J. Hu, C. Jiang, M. Ueda, X. Zhang, L. Wang, Positively charged  
506 nanofiltration membrane with dendritic surface for toxic element removal, ACS Sustainable  
507 Chem. Eng., 2017, **5**, 784-792.
- 508 32. X. Li, Y. Cao, G. Kang, H. Yu, X. Jie, Q. Yuan, Surface modification of polyamide  
509 nanofiltration membrane by grafting Zwitterionic polymers to improve the antifouling property,  
510 J. Appl. Polym. Sci., 2014, (1-9), DOI: 10.1002/APP.41144
- 511 33. J. Xu, Z. Wang, J. Wang, S. Wang, Positively charged aromatic polyamide reverse osmosis  
512 membrane with high anti-fouling property prepared by polyethylenimine grafting, Desalination,  
513 2015, **365**, 398-406.

- 514 34. C.X. Liu, D.R. Zhang, Y. He, X.S. Zhao, R. Bai, Modification of membrane surface for anti-  
515 biofouling performance: effect of anti-adhesion and anti-bacteria approaches, *J. Membr. Sci.*,  
516 2010, **346**, 121-130.
- 517 35. L. Setiawan, R. Wang, K. Li, A.G. Fane, Fabrication of novel poly(amide-imide) forward  
518 osmosis hollow fiber membranes with a positively charged nanofiltration-like selective layer, *J.*  
519 *Membr. Sci.*, 2011, **369**, 196-205.
- 520 36. J. Su, Y. Qiang J.F. Teo, T. Chung, Cellulose acetate nanofiltration hollow fiber membranes  
521 for forward osmosis processes, *J. Membr. Sci.*, 2010, **355**, 36-44.
- 522 37. W. N. A. S. Abdullah, W. Lau, F. Aziz, D. Emadzadeh, A.F. Ismail, Performance of  
523 nanofiltration-like forward-osmosis membranes for aerobically treated palm oil mill effluent,  
524 *Chem. Eng. Technol.*, 2018, **41**, 303-312
- 525 38. F. Fairbrother, H. Mastin, Studies in electro-endosmosis, Part I. *J. Chem. Soc., Transactions*,  
526 1924, **125**, 2319-2339.
- 527 39. D. Emadzadeh, W.J. Lau, A.F. Ismail, Synthesis of thin film nanocomposite forward osmosis  
528 membrane with enhancement in water flux without sacrificing salt rejection, *Desalination*, 2013,  
529 **330**, 90-99.
- 530 40. M. Seker, E. Buyuksari, S. Topcu, D. Seslib, D. Celebi, B. Keskinler, C. Aydiner, Effect of  
531 process parameters on flux for wheyconcentration with  $\text{NH}_3/\text{CO}_2$  in forward osmosis, *Food*  
532 *bioprod. Process*, 2017, **105**, 64-76.
- 533 41. C.Y. Wu, H. Mouri, S.S. Chen, D.Z. Zhang, M. Koga, J. Kobayashi, Removal of trace-  
534 amount mercury from wastewater by forward osmosis, *J. Water Process Eng.*, 2016, **14**, 108-116.

- 535 42. Horiba, Raman data and analysis, Raman Spectroscopy for Analysis and Monitoring,  
536 Application Note, 1-2.  
537 <http://www.horiba.com/fileadmin/uploads/Scientific/Documents/Raman/bands.pdf>
- 538 43. R. Lamsal, S.G. Harroun, C.L. Brosseau, G.A. Gagnon, Use of surface enhanced Raman  
539 spectroscopy for studying fouling on nanofiltration membrane, Sep. Purif. Technol., 2012, **96**, 7-  
540 11.
- 541 44. S. Cheng, D.L. Oatley, P.M. Williams, C.J. Wright, Positively charged nanofiltration  
542 membranes: Review of current fabrication methods and introduction of a novel approach, Adv.  
543 Colloid Interface Sci., 2011, **164**, 12-20.
- 544 45. R.N. Wenzel, Resistance of solid surfaces to wetting by water, Ind. Eng. Chem., 1936, **28**,  
545 988-994.
- 546 46. S. Zou, Y. Gu, D. Xiao, C.Y. Tang, The role of physical and chemical parameters on forward  
547 osmosis membrane fouling during algae separation, J. Membr. Sci., 2011, **366**, 356-362.
- 548 47. E.M. Vrijenhoek, S. Hong, M. Elimelech, Influence of membrane surface properties on  
549 initial rate of colloidal fouling of reverse osmosis and nanofiltration membranes, J. Membr. Sci.,  
550 2001, **188**, 115-128.
- 551 48. E.R. Cornelissen, D. Harmsen, K.F. de Korte, C.J. Ruiken, J.J. Qin, H. Oo, L.P. Wessels,  
552 Membrane fouling and process performance of forward osmosis membranes on activated sludge,  
553 J. Membr. Sci., 2008, **319**, 158-168.
- 554 49. W.A. Phillip, J.S. Yong, M. Elimelech, Reverse draw solute permeation in forward osmosis:  
555 Modeling and experiments, Environ. Sci. Technol., 2010, **44**, 5170-5176.

Table of contents entry:

Enhancing ammonium rejection by PEI modification

